Available online at www.sciencedirect.com
ScienceDirect
ELSEVIER
Energy 31 (2006) 3401–3414
ENERGY
www.elsevier.com/locate/energy

Analysis of a combined power and refrigeration cycle by the exergy method

A. Vidal[a,*], R. Best[b], R. Rivero[c,d], J. Cervantes[d]

[a]*Posgrado en Ingeniería (Energía), sede CIE-UNAM, Privada Xochicalco s/n, col. Centro, 62580, Temixco, Morelos, México*
[b]*Centro de Investigación en Energía, CIE-UNAM, Privada Xochicalco s/n, col. Centro, 62580, Temixco, Morelos, México*
[c]*Instituto Mexicano del Petróleo, Grupo de Exergia, Eje Central Lázaro Cárdenas No. 152, 07730, México D.F., México*
[d]*Facultad de Ingeniería, UNAM, Ciudad Universitaria, México D.F., México*

Abstract

The exergy analysis method was applied in order to evaluate the new combined cycle proposed by Goswami [Solar thermal technology: present status and ideas for the future. Energy Sources 1998;20:137–45], using Hasan–Goswami–Vijayaraghavan parameters. This new combined cycle was proposed to produce both power and cooling simultaneously with only one heat source and using ammonia–water mixture as the working fluid. The simulation of the cycle was carried out in the process simulator ASPEN Plus. The Redlich–Kwong–Soave equation of state was used to calculate the thermodynamic properties. The cycle was simulated as a reversible as well as an irreversible process to clearly show the effect of the irreversibilities in each component of the cycle. At the irreversible process two cases were considered, changing the environmental temperature. However, in order to know the performance of the new cycle at different conditions of operation, the second irreversible case was analyzed varying the rectification temperatures, the isentropic efficiency of the turbine and the return temperature of the chilled water. Exergy effectiveness values of ~53% and ~51% were obtained for the irreversible cycles; with heat input requirements at temperatures of 125 and 150 °C. Solar collectors or waste heat are suggested as heat sources to operate the cycle.

Keywords: Ammonia–water; Kalina cycle; Waste heat; Renewable energy; Aspen plus; Lorenz cycle

1. Introduction

In order to solve the problem of primary energy consumption in the energy systems and to reduce environmental pollution, new thermodynamic cycles have been investigated and developed during the past 20 yr [1]. Some of these new cycles were designed to operate with medium or low temperature heat sources, such as waste heat or renewable energy sources (e.g., geothermal) or the heat from solar collectors. Theoretical investigations show the potential of these new cycles to be operated with this kind of heat sources [2–5]. A characteristic of these new cycles is the use of environmentally friendly working fluids, i.e., ammonia–water mixture. In the early 1950s, this mixture was analyzed by Maloney and Robertson [6] to operate power cycles;

*Corresponding author. Tel.: +52 55 56 22 97 81; fax: +52 55 56 22 97 91.
E-mail address: avs@cie.unam.mx (A. Vidal).

0360-5442/$ - see front matter © 2006 Elsevier Ltd. All rights reserved.
doi:10.1016/j.energy.2006.03.001

Nomenclature

AB	absorber
ARM	absorption refrigeration machines
CHWI	chilled water inlet
CHWO	chilled water outlet
COWI	cooling water inlet
COWO	cooling water outlet
COP	coefficient of performance
CPC	compound parabolic concentrator
Efl	effluent exergy losses
$\dot{E}x$	exergy rate [kW]
GE	generator
h	enthalpy [kJ/kg]
HE	heat exchanger
$\dot{I}$	irreversibility rate [kW]
$\dot{m}$, MF	mass flow [kg/s]
MX	mixer
NA	not applicable/not available
P	pressure [bar]
Pot	improvement potential
$\dot{Q}$	heat rate [kW]
r	ratio of cooling to work net produced
RE	rectifier
s	entropy [kJ/kg K]
T	temperature [°C]
TV	throttle valve
VT	vapor turbine
$\dot{W}$	work output [kW]
X	ammonia weight percent

Greek letters

η	efficiency [%]
ε	exergy effectiveness [%]
Δ	gradient

Subscripts

0	environmental state
I	first law
II	second law
cool	cooler
cs	control surface
T	isentropic of turbine
L	Lorenz
np	net produced
ns	net supply
sh	shaft
sup	super

however, the major credit has been conceded to Kalina [7], who in 1983 proposed the use of this mixture as the working fluid in power cycles. To validate this research, pilot plants have been built, as combined power and refrigeration plants [8–11]. There is a worldwide interest to design energy systems that can work satisfactorily using less primary energy. Therefore, the trend is to produce integrated systems such as cogeneration and trigeneration systems, where both energy recovery and energy integration result in a higher thermodynamic efficiency than the separate simple systems.

In this context, a new combined cooling and power cycle was proposed by Goswami [3]. This was a combined cycle because it produced both power and cooling simultaneously with only one heat source, using ammonia–water mixture as the working fluid. Other researchers have also investigated this new cycle. Xu et al. [12] presented a parametric analysis of this cycle, Hasan et al. [13] applied an analysis of the first and second laws of thermodynamics to optimize the combined cycle. A characteristic of this new cycle is that the ammonia–water vapor that leaves the turbine passes through a heat exchanger (cooler) transferring only sensible heat; therefore, the produced cooling is relatively small. In order to produce a larger cooling effect, the working fluid should go through a phase change in the cooler. Zheng et al. [14] proposed a combined cycle utilizing Kalina′s technology [15] to condense the vapor before passing through the cooler, although the required heat source temperature was relatively high (350 °C). In a more recent work Zhang et al. [16] compare a cogeneration cycle based on ammonia–water with systems for separate power generation and refrigeration and show the advantages of the use of a binary mixture instead of pure fluids as working fluids. Later, Zhang and Lior [17] analyze several configurations of the cogeneration cycle and show the configuration with the highest energy and exergy efficiency. However, although these last cycles produce a larger refrigeration load, they were designed in order to operate with high temperature heat sources around 450 °C, out of the scope of this work.

In this paper the exergy analysis method was applied to evaluate the new combined cycle operated with low temperature heat sources proposed by Goswami. Exergy parameters were calculated such as second law efficiency, exergy effectiveness, effluent exergy losses, improvement potential and irreversibilities (exergy losses). The cycle was simulated as an irreversible process varying the isentropic efficiency of the turbine, which is different from the analysis presented by Hasan et al. [13], who assumed reversible behavior of the vapor turbine and solution pump. However, to compare the effect of the irreversibilities in these devices it was necessary to simulate both reversible and irreversible processes. The performance of the cycle was studied for two cases of environmental temperature, 17 and 25 °C; obtaining for the irreversible cases exergy effectiveness values of ~53% to ~51%, with heat requirements at temperatures of 125 and 150 °C. The exergy losses in each component of the cycle were also computed. The exergy analysis developed here shows the technical potential of the combined cycle to produce both electric and cooling energy even in the irreversible case.

2. Methods

2.1. Simulation and description of the combined power and refrigeration cycle

ASPEN Plus [18] was used to simulate the cycle and the Redlich—Kwong–Soave (RKS) equation of state was selected to calculate the thermodynamic properties of ammonia–water mixture because it shows good agreement with the literature [14,19] and experimental results obtained with an absorption prototype [20]. The following parameters and assumptions were used in the simulations: isentropic efficiency of the turbine (η_T) from 85% to 90%, isentropic efficiency of the pump 80%, mechanical and electric efficiency 96%, minimum temperature difference for each of the heat exchangers 5 °C, rectifier temperatures from 106 to 112 °C, chilled water inlet temperatures from 20 to 25 °C, reference temperatures, T_0, 17 and 25 °C, reference pressure, P_0, 1.0132 bar. The pressure drops were neglected in this analysis. The efficiency values for the turbine and pump and the temperature approach in the heat exchangers were based in the values suggested by Tamm et al. [11], Nag and Gupta [21] and Olsson et al. [22].

2.2. Cycle description

Fig. 1 shows the new cycle proposed by Goswami. The ammonia-strong saturated solution (1) which leaves the absorber (AB) is pumped to 20.5 bar (2). It is then split into two streams; stream 2A and stream 2B, the

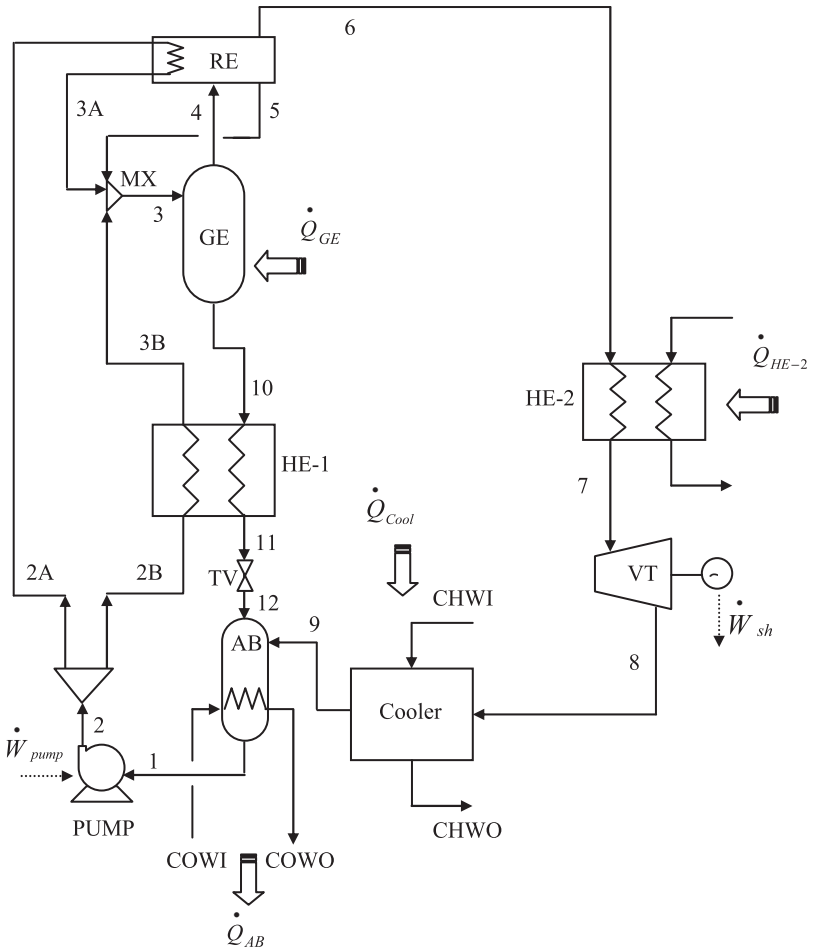

Fig. 1. Schematic diagram of the new combined cycle, adapted from Hasan et al. [13].

latter is preheated to 109 °C (3B) through the heat exchanger HE-1 by the ammonia-weak solution (10). Stream 2A is preheated to 93 °C (3A) through the rectifier (RE) by the rejected heat in this device. The condensed liquid (5) from the rectifier and both 3A and 3B streams are mixed in MX and then fed to the generator (3). In the generator (GE) which receives heat from a low temperature heat source, stream 3 is separated into an ammonia-weak solution (10) and an ammonia-rich vapor (4) which is purified in the rectifier. The ammonia-rich vapor (6) can be superheated through heat exchanger HE-2 and then be expanded through the turbine to produce power. The ammonia–water vapor (8) that leaves the turbine at low temperature (7 °C) passes through a cooler (9) providing cooling by sensible heat transfer to the chilled water. The ammonia-weak solution (11) coming from heat exchanger HE-1 passes through an expansion valve (TV) where it is throttled down to 2 bar (12). Both stream 12 and stream 9 are fed to the absorber to produce the ammonia-strong saturated solution (1) completing the cycle.

2.3. Exergy analysis method

The first law analysis method is widely used to evaluate thermodynamic systems; however, this method is concerned only with energy conservation, and therefore it cannot show how or where irreversibilities occur in a system or process. To determine the irreversibilities, the exergy analysis method is applicable, providing an indicator that points in which direction efforts should concentrate to improve the performance of the thermodynamic systems [23].

The maximum work obtainable from a system using the environmental parameters as reference state is called exergy and is expressible in terms of four components: physical exergy, kinetic exergy, potential exergy and chemical exergy. However, the kinetic and potential exergies are usually neglected and because there is no departure of chemical substances from the cycle to the environment, the chemical exergy is zero [24,25]. Therefore, in this analysis the physical exergy ($\dot{E}x$) is only considered and is calculated by the general expression:

$$= (h - h_0) - T_0(s - s_0), \tag{1}$$

where h and s are the enthalpy and entropy respectively and T_0 is the reference environmental temperature.

However, usually the analysis of a process requires of the difference in physical exergy for two states in the process rather than environmental state [24]. Therefore, from Eq. (1)

$$\dot{E}x = (h_1 - h_2) - T_0(s_1 - s_2). \tag{2}$$

Another form of exergy is associated with the heat transfer out of or into a control surface called thermal exergy ($\dot{E}x_Q$) defined as

$$\dot{E}x_Q = \dot{Q}\left(1 - \frac{T_0}{T_{cs}}\right), \tag{3}$$

where T_{cs} is the uniform temperature at the control surface.

2.4. Exergy balance and irreversibilities

Considering the control volume at steady state of Fig. 2 the exergy balance can be expressed as

$$\dot{E}x_{in} + \dot{E}x_{Q\,in} = \dot{E}x_{out} + \dot{E}x_{Q\,out} + \dot{W}_{sh} + \dot{I}, \tag{4}$$

where the subscripts in and out indicate inlets and outlets, respectively. The exergy losses due to irreversibilities in steady state can be determined for each component of the cycle by the following expression:

$$\dot{I} = T_0\left[\sum_{out} \dot{m}s - \sum_{in} \dot{m}s - \sum_{hs} \frac{\dot{Q}}{T_{hs}}\right], \tag{5}$$

where the first two terms represent the entropy flux associated with the flow of matter. The third term gives the sum of thermal entropy fluxes. With $\dot{Q} = 0$ the Eq. (5) can be written as:

$$\dot{I} = T_0\left[\sum_{out} \dot{m}s - \sum_{in} \dot{m}s\right]. \tag{6}$$

Eqs. (5) and (6) are known as the Gouy–Stodola relation and are applicable to all real process [24].

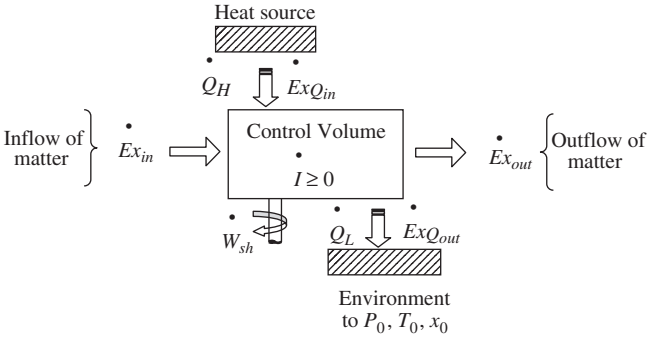

Fig. 2. Flow of matter and energy in a control region of a steady state process, adapted from Ref. [24].

2.5. Energy and exergy parameters

The first and second law efficiencies (Eqs. (7) and (8)) of the combined cycle were calculated by the definitions of Vijayaraghavan and Goswami [26]. The exergy parameters were calculated by the definitions of Rivero and Le Goff [27].

First law efficiency is obtained for the combined cycle by the following expression:

$$\eta_{\mathrm{I}} = \frac{\dot{W}_{\mathrm{np}} + \Delta\dot{\mathrm{E}}\mathrm{x}_{\mathrm{cool}}}{\dot{Q}_{\mathrm{GE}} + \dot{Q}_{\mathrm{supheat}}}, \tag{7}$$

where $\dot{W}_{\mathrm{np}}$ and $\Delta\dot{\mathrm{E}}\mathrm{x}_{\mathrm{cool}}$ are the net work and exergy changes of the chilled water in the cooler, respectively; produced by the combined cycle. $\dot{Q}_{\mathrm{GE}}$ and $\dot{Q}_{\mathrm{sup\ heat}}$ are the supply heat to generator and superheater, respectively.

The second law efficiency is a measure of the performance of a device relative to its performance under reversible condition. In the Goswami cycle the working fluid used is a zeotropic mixture of ammonia–water; therefore, the Lorenz cycle is used as reference cycle (reversible cycle) because is based on using a mixture of refrigerants as the working fluid rather than single pure refrigerant as the Carnot cycle [28]. The temperature–entropy diagram of the Lorenz cycle is shown in Fig. 3. Therefore, the expression in order to evaluate the second law efficiency can be written as:

$$\eta_{\mathrm{II}} = \frac{\eta_{\mathrm{I}}}{\eta_{\mathrm{rev}}}, \tag{8}$$

where the η_{rev} is based in the Lorenz cycle efficiency for power and refrigeration, which was developed by Vijayaraghavan and Goswami [26]:

$$\eta_{\mathrm{rev}} = \eta_{\mathrm{Lorenz}}\left[\frac{1+r}{1+\left(r/\mathrm{COP}_{\mathrm{Lorenz}}\right)}\right], \tag{9}$$

where η_{Lorenz} for power was developed as shown in Fig. 3a:

$$\eta_{\mathrm{Lorenz}} = 1 - \frac{(T_3 - T_4)/\ln(T_3/T_4)}{(T_2 - T_1)/\ln(T_2/T_1)}. \tag{10}$$

The $\mathrm{COP}_{\mathrm{Lorenz}}$ for refrigeration was developed as shown in Fig. 3b:

$$\mathrm{COP}_{\mathrm{Lorenz}} = \frac{(T_2 - T_1)/\ln(T_2/T_1)}{(T_3 - T_4)/\ln(T_3/T_4) - (T_2 - T_1)/\ln(T_2/T_1)}. \tag{11}$$

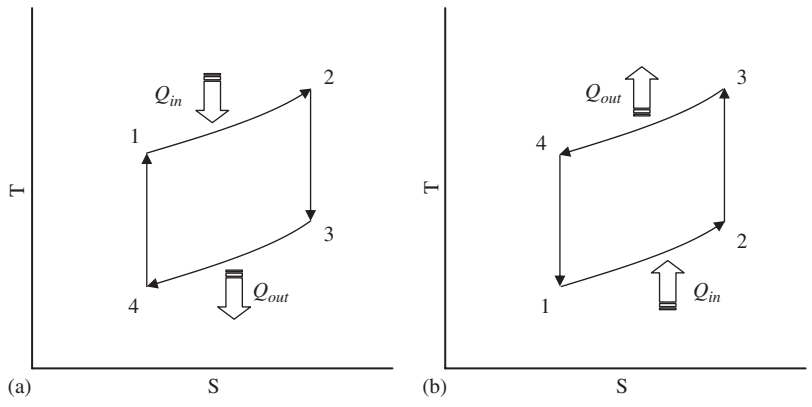

Fig. 3. (a) Temperature–entropy diagram for the Lorenz power cycle. (b) Temperature–entropy diagram for the Lorenz refrigeration cycle.

The ratio of cooling to work net produced (r) is

$$r = \frac{\dot{Q}_{\text{cool}}}{\dot{W}_{\text{np}}}. \tag{12}$$

The exergy effectiveness is defined as a measurement of the capacity of system to produce the desired effect, power and cooling in this case. The exergy effectiveness is calculated with the following expression:

$$\varepsilon = 1 - \frac{\dot{I}_{\text{Cycle}}}{\dot{\text{E}}\text{x}_{\text{ns}}} = \frac{\dot{\text{E}}\text{x}_{\text{np}}}{\dot{\text{E}}\text{x}_{\text{ns}}} = \frac{\dot{W}_{\text{sh}} + \Delta\dot{\text{E}}\text{x}_{\text{CW}}}{\Delta\dot{\text{E}}\text{x}_{\text{GE}} + \Delta\dot{\text{E}}\text{x}_{\text{HE-2}} + \dot{W}_{\text{pump}} - \Delta\dot{\text{E}}\text{x}_{\text{AB}}}, \tag{13}$$

where $\dot{\text{E}}\text{x}_{\text{np}}$ and $\dot{\text{E}}\text{x}_{\text{ns}}$ are the net exergy produced and net exergy supplied, respectively; $\Delta\dot{\text{E}}\text{x}_{\text{CW}}$, $\Delta\dot{\text{E}}\text{x}_{\text{GE}}$, $\Delta\dot{\text{E}}\text{x}_{\text{HE-2}}$ and $\Delta\dot{\text{E}}\text{x}_{\text{AB}}$ are the exergy changes of chilled water, heating fluid (in the generator and superheater) and cooling water or cooling air (in the absorber), respectively. $\Delta\dot{\text{E}}\text{x}_{\text{GE}}$ and $\Delta\dot{\text{E}}\text{x}_{\text{HE-2}}$ were computed by the definition of thermal exergy given by Eq. (3), because the heat sources in the generator and the superheater are not yet defined.

The effluent exergy losses are the sum of all exergy streams rejected to the environment. For the combined cycle analyzed the absorber heat is the only stream rejected to the environment; therefore

$$\text{Efl} = \Delta\dot{\text{E}}\text{x}_{\text{AB}}. \tag{14}$$

The exergy analysis would not be complete if it is not known how much the efficiency or effectiveness of a system or processes could be improved. The improvement potential of a system is a measure of how much and how easily the system could be improved for optimization purposes and can be obtained by the following expression:

$$\text{Pot} = \dot{I}_{\text{Cycle}}(1 - \varepsilon) + \text{Efl}. \tag{15}$$

The first term of Eq. (15) has been proposed by van Gool, cited by Hammond et al. [29], to define the improvement potential; however, Rivero et al. [27] added the term of environmental potential (Efl), which is a measure of how much a system can be improved by using the effluent streams instead of rejecting their exergy to the surrounding medium. This term has a greater importance when the temperature level of effluents is high; so their recovery is feasible.

3. Results and discussion

To consider the operation of the turbine and the pump as reversible in a thermodynamic analysis can be useful only as an idealized reference point, since the real behavior of these devices is very far from reversible. Therefore, in order to be able to improve a process it is necessary to know the nature of the irreversibilities. It is important to mention that considering in the simulation the turbine as a reversible device leads to that the fluid coming out of the steam turbine is at a low temperature, which produces cooling by passing it through a heat exchanger, as reported by Hasan et al. [13]; however, considering the turbine as irreversible the cooling effect is diminished for the reasons that are explained in the following paragraphs. Therefore, in this work it was investigated how the production of power and cooling of the Goswami cycle is affected when simulated in a more realistic way; considering for the pump and turbine isentropic and mechanical efficiencies, common in the operation and design as reported in the literature [11]. The rectification temperatures and the return temperatures of the chilled water also were varied in this analysis.

At the beginning of this investigation, the operation parameters reported in the work of Hasan et al. [13] were used in our simulation, changing only the efficiencies in the pump and the turbine (first irreversible case). Under these conditions, the result was that the fluid that leaves the turbine resulted in greater temperature (17.8 °C) than the environmental temperature (17 °C); therefore, the cooling effect was null. It was necessary to lower P_{out} (1.5 bar) to obtain the suitable temperature to reach the cooling effect. However, this decrease of P_{out} leads to absorber temperatures lowers than the environmental temperature, which could make it difficult to reject the absorption heat. Therefore, the operation parameters were modified to reach, in addition to produced power, useful cooling. The environmental temperature was changed from 17 to 25 °C, the P_{out} was increased from 2 to 3.15 bar, in order to guarantee that the absorption heat can be rejected with water or air to

Table 1
Parameters obtained in the simulation of the first irreversible case ($T_0 = 17\,C$, $\eta_T = 85\%$)

Stream	T [°C]	P [bar]	h [kJ/kg]	S [kJ/kg K]	$\dot{m}$ [kg/s]	X (kg NH_3/kg H_2O) [%]	Ėx [kW]
1	9.72	1.50	−11024.0	−10.53327	1	43.70	9.70
2	9.87	20.50	−11021.0	−10.53326	1	43.70	12.69
2A	9.87	20.50	−11021.0	−10.53326	0.05	43.70	0.69
2B	9.87	20.50	−11021.0	−10.53326	0.95	43.70	12.00
3	103.89	20.50	−10529.0	−9.026655	1.00	43.66	73.94
3A	110.00	20.50	−10423.0	−8.762368	0.05	43.70	5.32
3B	103.48	20.50	−10530.0	−9.043041	0.95	43.70	67.62
4	125.00	20.50	−3355.8	−6.352111	0.18	92.30	83.39
5	108.50	20.50	−10913.0	−8.960369	0.01	40.42	0.91
6	108.50	20.50	−2963.9	−6.64026	0.17	96.30	74.07
7	108.50	20.50	−2963.9	−6.640266	0.17	96.30	74.07
8	6.74	1.50	−3283.7	−6.434268	0.17	96.30	9.08
9	12.00	1.50	−3260.6	−6.352584	0.17	96.30	8.97
10	125.00	20.50	−11734.0	−8.609784	0.83	32.83	71.16
11	14.87	20.50	−12294.0	−10.25295	0.83	32.83	1.97
12	15.30	1.50	−12294.0	−10.24326	0.83	32.83	−0.35
CHWI	17.00	1.50	−15899.0	−9.169373	0.18	0.00	0.00
CHWO	11.73	1.50	−15921.0	−9.246064	0.18	0.00	0.02
COWI	4.72	1.50	−15950.0	−9.350442	13.19	0.00	12.97
COWO	9.72	1.50	−15912.0	−9.275608	13.19	0.00	8.90

Table 2
Parameters obtained in the simulation of the second irreversible case ($T_0 = 25\,C$, $\eta_T = 85\%$)

Stream	T [°C]	P [bar]	h [kJ/kg]	s [kJ/kg K]	$\dot{m}$ [kg/s]	X (kg NH_3/kg H_2O) [%]	Ėx [kW]
1	30.07	3.15	−10922.00	−10.18744	1.00	43.70	18.38
2	30.33	30.00	−10918.00	−10.18729	1.00	43.70	22.34
2A	30.33	30.00	−10918.00	−10.18729	0.17	43.70	3.85
2B	30.33	30.00	−10918.00	−10.18729	0.83	43.70	18.49
3	129.10	30.00	−10282.00	−8.54586	1.05	44.10	127.48
3A	135.00	30.00	−10250.00	−8.34344	0.17	43.70	24.25
3B	129.33	30.00	−10335.00	−8.55206	0.83	43.70	97.72
4	150.00	30.00	−3804.00	−6.23371	0.24	87.80	123.49
5	108.00	30.00	−9546.80	−9.15048	0.05	51.74	4.90
6	108.00	30.00	−2812.80	−6.95997	0.18	97.95	88.50
7	120.00	30.00	−2780.90	−6.87758	0.18	97.95	89.85
8	11.31	3.15	−3057.10	−6.70351	0.18	97.95	29.48
9	20.00	3.15	−3020.20	−6.57584	0.18	97.95	29.26
10	150.00	30.00	−11761.00	−8.26123	0.82	31.46	92.48
11	35.33	30.00	−12353.00	−9.88781	0.82	31.46	4.95
12	35.91	3.15	−12353.00	−9.87486	0.82	31.46	1.80
CHWI	25.00	1.50	−15866.00	−9.05579	0.19	0.00	0.00
CHWO	16.31	1.50	−15902.00	−9.17929	0.19	0.00	0.15
COWI	25.00	1.50	−15866.00	−9.05579	13.74	0.00	0.20
COWO	30.00	1.50	−15845.00	−8.98639	13.74	0.00	4.57

the environmental temperature. The operation temperature also was increased from 125 to 150 °C (second irreversible case). The exergy analysis was carried out using the data produced in the simulations; only two simulation cases are reported in Tables 1 and 2.

Table 3 shows the comparison of the thermodynamic parameters for the reversible and both irreversible cases, the reversible case is only added as an ideal reference. In the second irreversible case, with higher T_0, the power produced was 7.2% less than the first irreversible case, causing also a decrease in the first law efficiency

Table 3
Comparison of thermodynamic parameters

Parameters	Reversible cycle (Hasan et al. [13])	Irreversible cycles [this work]	
	$T_0 = 17\,^{\circ}C$	$T_0 = 17\,^{\circ}C$	$T_0 = 25\,^{\circ}C$
$\dot{W}_{sh}$ (kW)	49.4[a]	52.6[b]	48.8[b]
$\dot{W}_{pump}$ (kW)	2.2	3.0	4.4
$\dot{Q}_{cool}$ (kW)	3.5	4.0	6.8
$\dot{Q}_{GE\ in}$ (kW)	278.8	324.5	320.3
$\dot{Q}_{Supheat\ in}$ (kW)	0.0	0.0	5.9
$\dot{Q}_{AB\ out}$ (kW)	235.2	277.0	287.0
η_I (%)	16.9	15.3	13.7
η_{rev} (%)	25.8	27.0	27.8
COP_L	NA	6.0	5.6
η_L (%)	NA	25.4	24.81

[a]Turbine efficiency = 100%.
[b]Turbine efficiency = 85%.

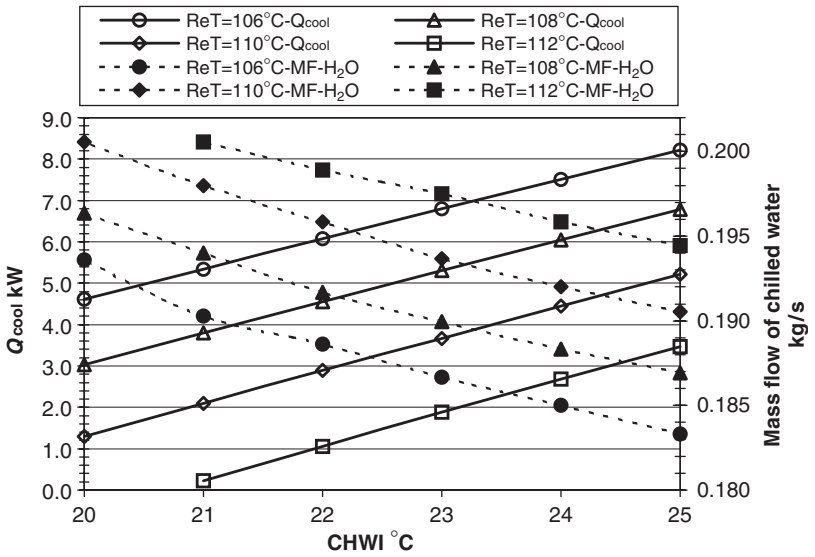

Fig. 4. Cooling load and mass flow of chilled water produced versus inlet temperatures of chilled water in the cooler, for an isentropic efficiency of the turbine of 85% and for four rectifier temperatures.

of 10.5%, falling from 15.3% to 13.7%. This decrease in the power output is due to the high P_{out} of the turbine, which by environmental conditions was set at 3.15 bar. It was also necessary to add 5.9 kW of superheating in this case. The cooling produced was 4.0 and 6.8 kW for the first and the second irreversible cases, respectively. This increase of the cooling load, for the second irreversible case, was because the temperature change of the chilled water stream (ΔT) was higher (8.7 °C) than the first irreversible case (5 °C). However, it is unlikely that the chilled water returns to the environment temperature; therefore, the return temperature of chilled water was varied from 25 to 20 °C in order to know the behavior of the cooling load and mass flow of chilled water produced. Fig. 4 shows the results of these variations; the cooling load is decreased as the return temperature of the chilled water is also decreased. However, this decrease in the cooling load is more noticeable for high rectification temperatures, because the refrigerant stream does not have the ammonia

Table 4
Exergy parameters

Parameters	Reversible cycle[a] $T_0 = 17\,^{\circ}C$	Irreversible cycle[b] $T_0 = 17\,^{\circ}C$	Irreversible cycle[b] $T_0 = 25\,^{\circ}C$
η_{II} (%)	65.4	56.5	49.2
ε (%)	NA	52.4	51.0
Efl (kW)	NA	−9.3	4.4
Pot (kW)	NA	13.5	27.5
$\dot{I}_{Cycle}$ (kW)	25.3	48.0	47.0

[a]Turbine efficiency = 100%.
[b]Turbine efficiency = 85%.

purity necessary to obtain low temperatures in the cooler. Fig. 4 is also useful to know the mass flow of chilled water for different conditions.

Table 4 shows the exergy parameters for both reversible and irreversible cases. In the second irreversible case, the second law efficiency (η_{II}) and the exergy effectiveness (ε) diminished 12.9% and 2.7%, falling from 56.5% to 49.2% and from 52.4% to 51.0%, respectively, with respect to the first irreversible case. This decrease is due to the fact that the first irreversible cycle "can produce more exergy" ($\dot{W}_{sh} + \Delta\dot{E}x_{cool}$) than the second irreversible cycle, although it is true thermodynamically, an additional cooling system would be necessary in order to have a correct operation. Although in the irreversible cases there is a high entropy generation, there is also a high improvement potential (Pot), 27.5 and 13.5 kW, which means that applying optimization techniques and using very efficient devices, the total irreversibility of the cycles could be reduced and consequently the exergy effectiveness of the cycle could be increased. Substituting values of Table 3 and Table 4 in Eqs. (13)–(15); the cycle irreversibility, 47.1 and 47.7 kW, could be reduced up to 19.6 and 34.6 kW for the second and the first irreversible case, respectively. Consequently the exergy effectiveness could be increased up to 79.8% and 65.5% for the second and the first irreversible case, respectively. The effluent exergy losses (Efl) were negative in the first irreversible case because the absorption temperature (9.7 °C) was lower than the ambient temperature (17 °C). Therefore, in order to reach the condensation of the solution it would be necessary to cool the absorber with water or air at a temperature below 9.7 °C. In this work for the first irreversible case, cooling water inlet temperature was assumed at 4.7 °C and the outlet temperature at 9.7 °C, in order to remove the absorption heat and to obtain the ammonia-strong solution. As the streams were below the ambient temperature, the exergy losses were negative. However, this case is not considered feasible due to the amount of chilled water required. The specifications of these streams are shown in Table 1. In the second irreversible case this problem was solved increasing P_{out} to 3.15 bar, but increasing also the operation temperature to 150 °C. However, the cycle efficiency was diminished due the exergy produced was lower respect to the exergy supply. In this second irreversible case, the cycle efficiency can be improved, amongst other ways by improving the efficiency of the turbine.

As the cooling produced by the cycle is an important factor in the possible use of the cycle, it is of interest to analyze how to increase the cooling capacity produced. For a fixed generation temperature of 150 °C, producing an ammonia vapor of higher purity can increase the cooling capacity. This is achieved by reducing the rectifier operating temperature. Fig. 5a shows the reduction in refrigerant vapor temperature entering the cooler as function of the isentropic efficiency of the turbine (η_T) for four rectifier temperatures. The corresponding ammonia vapor concentration in weight percent is also shown. It can be seen that for an isentropic efficiency of 85%, the refrigerant vapor temperature entering the cooler decreases by 6 °C when the rectifier temperature is reduced from 112 to 106 °C. The same temperature difference is maintained as the isentropic efficiency of the turbine is increased, although at lower refrigerant temperatures. This produces, as shown in Fig. 5b, an increasing in the cooling load, which is more noticeable as the turbine efficiency increases and as the rectifier temperature decreases.

Fig. 6 shows the behavior of the second law efficiency and of the exergy effectiveness. As expected, the exergy parameters decrease as the rectifier temperature decrease. Producing a higher purity refrigerant in the

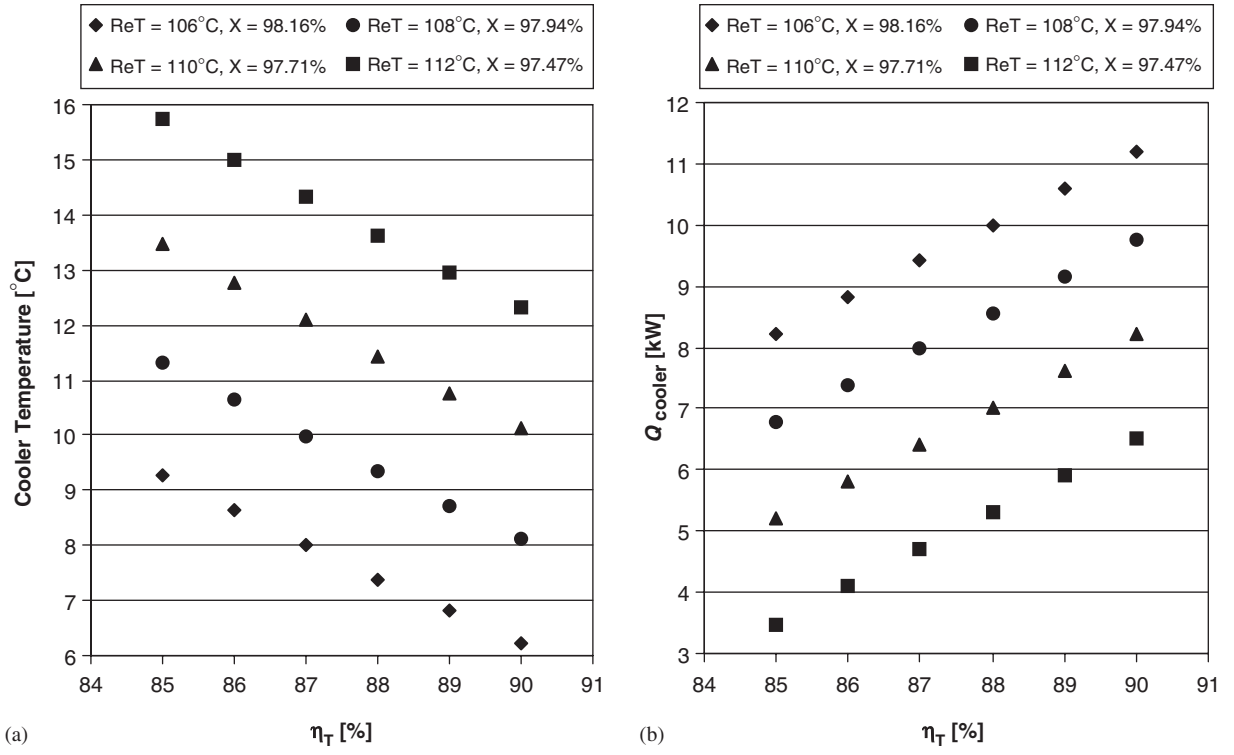

Fig. 5. (a) Reduction of the refrigerant vapor temperature entering the cooler versus the isentropic efficiency of the turbine (η_T). (b) Increase in the cooling load versus η_T for four rectifier temperatures.

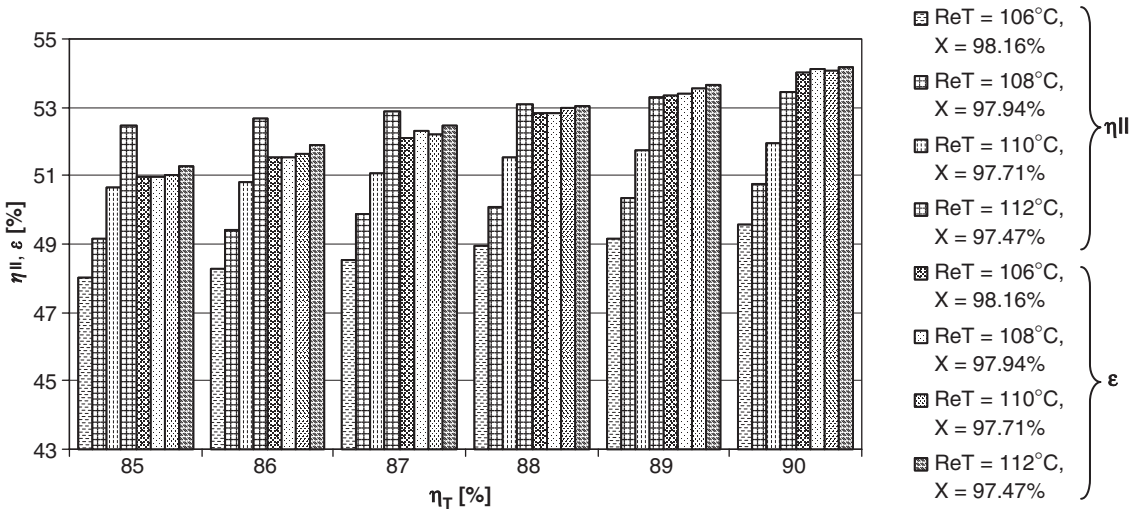

Fig. 6. Behavior of the second law efficiency and of the exergy effectiveness, as the isentropic efficiency of the turbine and the rectifier temperature are increased.

rectifier increases the temperature difference between generator and rectifier and more heat is needed in the superheater.

Fig. 7a shows, for the second irreversible case, a lowering of the total irreversibility of the cycle by 0.5 kW, as the rectifier temperature is decreased from 112 to 106 °C. This behavior is higher if the isentropic efficiency

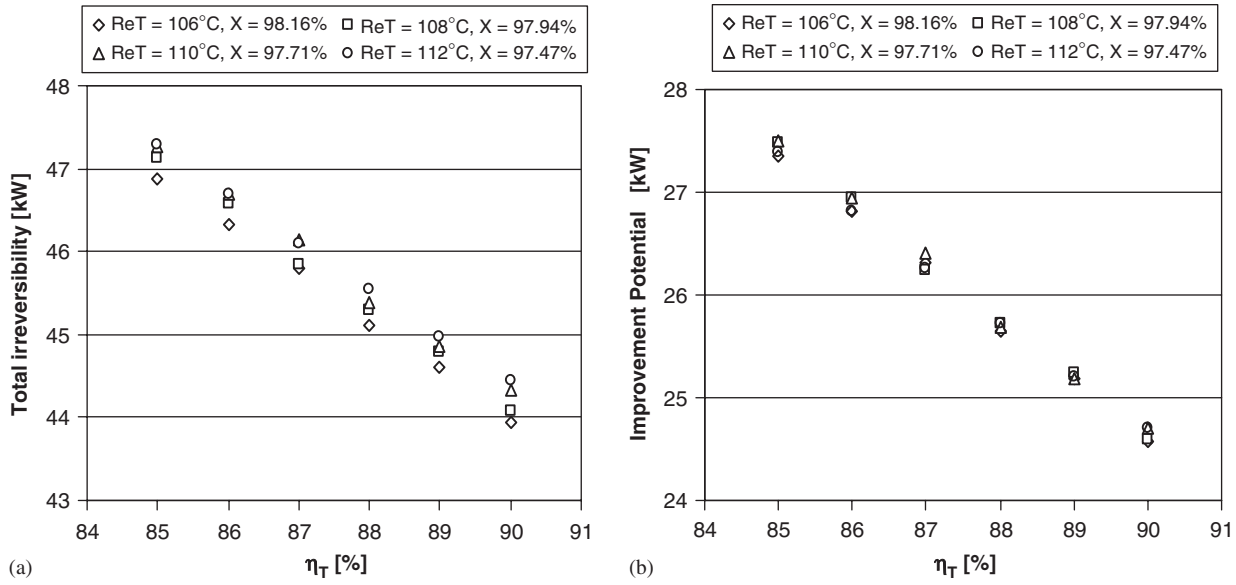

Fig. 7. (a) Decrease of the total irreversibility versus the isentropic efficiency of the turbine (η_T). (b) Improvement potential versus η_T for four rectifier temperatures.

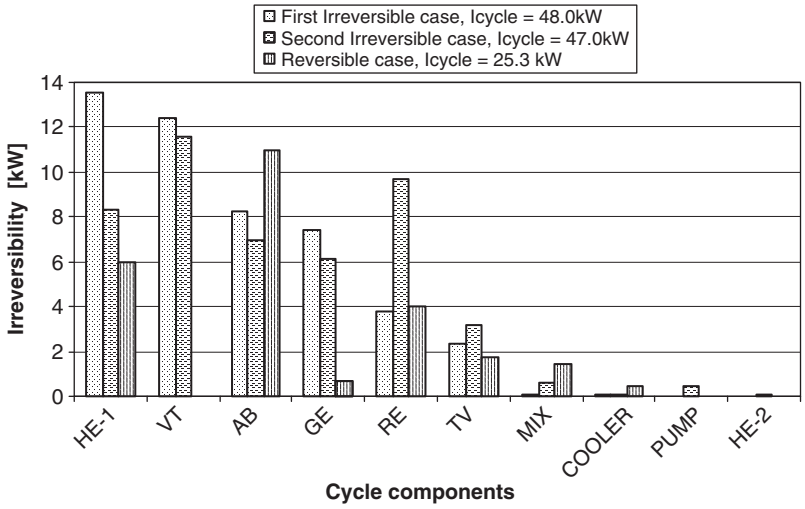

Fig. 8. Irreversibilities of each component of the cycle for the reversible and irreversible cases.

of the turbine is increased. As Fig. 7b shows, the lowering of total irreversibility is reflected in the decrease of the improvement potential.

Fig. 8 shows the irreversibilities of each component of the cycle for the reversible and irreversible cases. For the first irreversible case the component with the highest irreversibility was the heat exchanger (HE-1) with 13.6 kW with respect to 8.3 kW of second irreversible case; because in this last case the stream 3B reaches a higher vapor fraction; therefore, it also has a higher exergy value. For both irreversible cycles, the turbine (VT) resulted with irreversibilities of 12.4 and 11.6 kW (25.9% and 24.6% of the total irreversibility) for the first and second case, respectively, due to the assumed isentropic efficiency of 85%. However, it is well known that increasing the turbine efficiency, the irreversibility in this device is reduced. For the second irreversible case the irreversibility in the turbine was diminished by 11, 10.4, 9.8, 9.2 and 8.5 kW for isentropic efficiencies set at:

86%, 87%, 88%, 89% and 90%, respectively. The absorber (AB) resulted with 8.3 and 6.9 kW (17.2% and 14.7% of the total irreversibility), the generator (GE) resulted with 7.5 and 6.2 kW (15.5% and 13.1% of the total irreversibility) for first and second case, respectively. Although in these devices both mass and heat transfer processes causes more entropy generation, the high irreversibility is due mainly to the heat transfer process [23]. In the rectifier (RE) the irreversibility was 3.8 and 9.7 kW (7.9% and 20.6% of the total irreversibility) for first and second case, respectively, due to the temperature gradient between the generator and the rectifier. The irreversibility in this device increases or reduces as the rectification temperature is diminished or increased. For the second irreversible case the irreversibility in the rectifier varied by: 9.9, 9.4 and 9.1 kW for rectification temperatures of: 106 °C ($X = 98.16\%$), 110 °C ($X = 97.71\%$) and 112 °C ($X = 97.47\%$), respectively and for an efficiency $\eta_T = 85\%$. Therefore, in order to reduce the entropy generation in this device, it should be designed with the maximum effectiveness. This also applies to HE-1, which plays an important role in the optimization of the cycle; although this would increase the size and price of the system. Other key parameters to reduce the irreversibility and optimize the absorption cycle have been discussed by other authors. Aphornratana and Eames [23] proposed to reduce the solution circulation rate and to use a more effective solution heat exchanger (HE-1). Vicatos and Gryzagoridis [30], Tamm et al. [11] proposed to optimize the generator temperature to reduce the entropy generation and to reach a better performance of the cycle. The other components of the cycle resulted with smaller irreversibilities; however, they must be taken into account for a good cycle optimization.

Heat sources for driving the combined cycle can be obtained from the waste heat rejected by the furnaces, boilers or some streams of processes having temperatures between 150 and 300 °C [5,31]. The heat from solar collectors also can be used, e.g., Krüger et al. [32] proposed to use parabolic trough collectors to drive absorption cooling machines (ACM) of single and double effect. Direct steam generation into solar power systems has been technically proven and analyzed up to temperatures of 400 °C, with parabolic trough collectors or utilizing Fresnel reflectors [33,34]. Ortega and Best [4] proposed a compound parabolic concentrator (CPC) for the direct vapor generation in an ammonia–water absorption solar refrigerator, e.g., a CPC acts as the generator in absorption refrigeration cycle in which an input temperature of 60 °C, an output of 108 °C and initial ammonia concentration of 39% are achieved in the simulation. Higher generating temperatures required in the combined power and cooling cycle analyzed could be achieved with CPC technology.

4. Conclusions

The exergy analysis method applied to a new cycle shows its potential to produce both power and cooling using heat sources at low temperature, even for the irreversible cycles. However, the cooling produced is small as compared to the generated power. With reference to the system proposed by Goswami, the cycle was analyzed, varying some important set points, such as the ambient temperature, turbine efficiency and rectifier temperature. Exergy parameters were good indicators to show the effectiveness of the cycle, as well as to identify the devices where most exergy destruction occurs. Although in the irreversible cycles there is a high entropy generation, there is also a high improvement potential, which means that applying optimization techniques, the total irreversibility of the cycle could be reduced.

Acknowledgments

The authors thank the financial support for this research work, through of PAPIT Project IN105602-3 and CONACYT Project U44764-Y. Discussions in order to improve the work presented in this paper came from a post-graduate course (Redacción de artículos en ciencias e ingenierías) offered by Surendra Pal Verma, which was attended by the first author (A. Vidal). We are also grateful to Victor H. Gómez for useful discussions.

References

[1] Goswami DY, Vijayaraghavan S, Lu S, Tamm G. New and emerging developments in solar energy. Sol Energy 2004;76(1–3):33–43.

[2] Marston CH, Sanyal Y. Optimization of Kalina cycles for geothermal application. AES 1994;33:97–104.
[3] Goswami DY. Solar thermal technology: present status and ideas for the future. Energy Sources 1998;20:137–45.
[4] Ortega N, Best R. Modeling of a compound parabolic concentrator with direct vapor generation for refrigeration applications. In: Eleventh SolarPACES international symposium on concentrated solar power and chemical energy technologies, Zurich, Switzerland. 2002.
[5] Vidal A. Estudio sobre la operación de sistemas de refrigeración por absorción avanzados con fuentes de calor residual y renovable. PhD. thesis, Centro de Investigación en Energía de la Universidad Nacional Autónoma de México. Temixco, Morelos, México, 2005 (in process).
[6] Maloney JD, Robertson RC. Thermodynamic study of ammonia–water heat power cycles. Report CF-53-8-43. Oak Ridge National Laboratory Oak Ridge, TN 3783, Roane County, TN, 1953.
[7] Kalina AI. Combined cycle and waste-heat recovery power systems based on a novel thermodynamic energy cycle utilizing low-temperature heat for power generation. American Society of Mechanical Engineers Paper 1983; 83-JPGC-GT-3.
[8] Kalina AI, Leibowitz H. The design of a 3 MW Kalina cycle experimental plant. American Society of Mechanical Engineers Paper 1988; Amsterdam 88-Gt-140.
[9] Leibowitz H. Operating experience on the 3 MW Kalina cycle demonstration plant. In: Proceedings of the American power conference, Chicago. 1993.
[10] Velázquez N. Estudio de sistemas de absorción avanzados para operar con gas natural asistido por energía solar. PhD. thesis, Universidad Nacional Autónoma de México, México D.F., 2002.
[11] Tamm G, Goswami DY, Lu S, Hasan AA. Theoretical and experimental investigation of an ammonia–water power and refrigeration thermodynamic cycle. Sol Energy 2004;76(1–3):217–28.
[12] Xu F, Goswami DY, Bhagwat SS. A combined power/cooling cycle. Energy 2000;25(3):233–46.
[13] Hasan AA, Goswami DY, Vijayaraghavan S. First and second law analysis of a new power and refrigeration thermodynamic cycle using a solar heat source. Sol Energy 2002;73(5):385–93.
[14] Zheng D, Chen B, Qi Y. Thermodynamic analysis of a novel absorption power/cooling combined cycle. In: International sorption heat pump conference, Shanghai, China. 2002.
[15] Kalina AI, Leibowitz HM. Appling Kalina technology to a bottoming cycle for utility combined cycles. American Society of Mechanical Engineers Paper 1987, 87-GT-35.
[16] Zhang N, Cai R, Lior N. A novel ammonia–water cycle for power and refrigeration cogeneration. In: Proceedings of IMECE04, ASME international mechanical engineering congress and exposition, Anaheim, CA, USA. Paper IMECE 2004-60692, 2004.
[17] Zhang N, Lior N. Configuration selection methodology for combined power/refrigeration generation ammonia–water cycles. In: Proceedings of ECOS 2005, Trondheim, Norway. 2005.
[18] Aspen Plus, version 12.1. 2004. Aspen Technology, Inc. Ten Canal Park, Cambridge, MA, USA, www.aspentech.com.
[19] Bogart MJP. Ammonia absorption refrigeration industrial processes. Houston, TX: Gulf Professional Publishing Company; 1981.
[20] Gómez VH, Vidal A, García C, García-Valladares O, Best R, Hernández J, Velázquez N. Evaluation of an indirect-fired gas cycle cooling system. In: International sorption heat pump conference 2005, Denver, Colorado. Paper ISHPC-004-2005.
[21] Nag PK, Gupta AVSSKS. Exergy analysis of the Kalina cycle. Appl Therm Eng 1998;18(6):427–39.
[22] Olsson EK, Thorin EB, Dejfors CAS, Svedberg G. Kalina cycles for power generation from industrial waste heat. In: FLOWERS′94—Florence world energy research symposium, Florence, Italy. 1994.
[23] Aphornratana S, Eames IW. Thermodynamic analysis of absorption refrigeration cycles using the second law of thermodynamic method. Int J Refrig 1995;18(4):244–52.
[24] Kotas TJ. The exergy method of thermal plant analysis. Malabar, FL: Krieger Publish Company; 1995.
[25] Moran MJ. Fundamentals of energy analysis and exergy-aided thermal systems design. In: Bejan A, Mamut E, editors. Thermodynamic optimization of complex energy systems. Dordrecht, The Netherlands:Kluwer Academic Publishers;p. 73–92.
[26] Vijayaraghavan S, Goswami DY. On evaluating efficiency of a combined power and cooling cycle. ASME J Energy Resour Technol 2003(125):221–7.
[27] Rivero R, Le Goff P. On the performance criteria of sorption heat pumps and heat transformer. In: Efficiency, costs, optimization and simulation of energy systems. New York:American Society of Mechanical Engineers;1992. p. 575–86.
[28] McMullan JT, Morgan R. Heat pumps. Great Britain: Adam Hilger Ltd.; 1981.
[29] Hammond GP, Stapleton AJ. Exergy analysis of the United Kingdom energy system. Proc Inst Mech Eng A: J Power Energy 2001;215(A2):141–62.
[30] Vicatos G, Gryzagoridis J. The role of the heat exchanger in the design and optimization of the absorption refrigeration machines. In: Proceedings of absorption'96, Montreal. 1996. p. 361–6.
[31] Olszewsky M. Utilization of reject heat. New York and Basel: Mitchell editorial Marcel Dekker, Inc.; 1989.
[32] Krüger D, Pitz-Paal R, Lokurlu A, Rcharts F. Solar cooling and heating with parabolic trough collectors for a hotel in the Mediterranean. In: Eleventhth SolarPACES international symposium on concentrated solar power and chemical energy technologies, Zurich, Switzerland. 2002.
[33] Rheinländer J, Marquand-Mollenstadt T, Gräter F. Integration of direct steam generation into solar electric power systems—advanced commercial software for energy performance analysis. In: Eleventh SolarPACES international symposium on concentrated solar power and chemical energy technologies, Zurich, Switzerland. 2002. p. 599–605.
[34] Solarmundo, 2004, http://www.solarmundo.be/.